Chemical Engineering Journal 273 (2015) 656–667

Contents lists available at ScienceDirect

Chemical Engineering Journal

journal homepage: www.elsevier.com/locate/cej

Gas to liquid mass transfer in rheologically complex fluids

Y. Bajón Fernández [a], E. Cartmell [a,*], A. Soares [a], E. McAdam [a], P. Vale [b], C. Darche-Dugaret [c], B. Jefferson [a]

[a] Cranfield Water Science Institute, School of Applied Sciences, Cranfield University, Cranfield, Bedfordshire MK43 0AL, UK
[b] Severn Trent Water, 2 St John's Street, Coventry CV1 2LZ, UK
[c] Ecole Nationale Supérieure de Chimie de Rennes, 11 Allée de Beaulieu, 35708 Rennes Cedex 7, France

HIGHLIGHTS

- The impact of μ_a on mass transfer was studied for different liquid rheologies.
- Reduction of k_La with μ_a was non-linear for Newtonian and non-Newtonian fluids.
- Impact of μ_a and U_G in k_La was predominantly influenced by changes in hydrodynamics.
- Slug–annular flow was formed in shear thinning fluids, with a reduced active volume.
- Rheology and μ_a need to be considered in design of sludge mass transfer systems.

ARTICLE INFO

Article history:
Received 1 October 2014
Received in revised form 15 February 2015
Accepted 10 March 2015
Available online 19 March 2015

Keywords:
Mass transfer
Viscous fluids
Anaerobic digestion

ABSTRACT

The increase of studies relaying on gas to liquid mass transfer in digested sludge (shear thinning fluid) necessitates a better understanding of the impact of apparent viscosity (μ_a) and rheology in process performance. Mass transfer retardation due to μ_a variations was investigated in a pilot scale absorption bubble column for Newtonian and shear thinning fluids with varied superficial gas velocities (U_G). A non-linear reduction of mass transfer efficiency with increasing μ_a was observed, being the impact higher at low μ_a ranges and high U_G. An increase of 114 cPo in μ from 1.01 to 115 cPo in glycerol solutions saturated with U_G = 1.73 cm s^{-1} led to a reduction of 96% in k_La (α = 0.04), while a comparable raise from 115 to 229 cPo implied a reduction of 52% (α = 0.02).

Slug–annular flow regime was identified for shear thinning fluids of high μ_a (1.0% and 1.5% carboxymethyl cellulose sodium salt solutions), where bubble buoyancy was conditioned by the μ of the fluid at rest and the active volume for mass transfer was reduced because of the presence of stagnant areas. Conditions imitating the rheological variability of anaerobically digested sewage sludge were included within those tested, being a reduction in gas transfer efficiency of 6 percentage points (from 7.6 ± 0.3% to 1.6 ± 0.1%) recorded when increasing μ_a from 130 to 340 cPo. It is thus recommended that rheology and μ_a variability are accounted for within the design of gas to liquid mass transfer systems involving digested sewage sludge, in order to avoid reductions in process performance and active volume.

1. Introduction

Unit processes that utilise mass transfer in gas–liquid systems are widely used in both the environmental and industrial sectors in processes such as polyester production [1], fermentation broths cultivation [2], xanthan gum production [3] and wastewater treatment. The fluids being considered are often of non simple rheology and exhibit localised variation in viscosities (μ) making understanding of such systems difficult. A recent new area of consideration relates to the anaerobic digestion of organic waste and municipal wastewater in processes such as ammonia stripping from digestate to reduce toxicity [4], and carbon dioxide (CO_2) enrichment of sewage sludge or food waste for enhanced biogas production and carbon uptake [5]. For instance, sewage sludge is

Abbreviations: AD, anaerobic digester; C, concentration in the liquid phase; C^*, solubility as equilibrium CO_2 concentration at infinite time; C_0, concentration at time zero; C_t, concentration at time t; C_{model}, concentration estimated with Eq. (5); C_{sensor}, concentration measured by the probe; CMC, carboxymethyl cellulose sodium salt; $\dot{F}_{CO_2}$, incoming CO_2 mass flow rate; GTE, gas transfer efficiency; GTR, gas transfer rate; K, consistency index; k_La, volumetric mass transfer coefficient; $(k_La)_T$, volumetric mass transfer coefficient at temperature T; $(k_La)_{20}$, volumetric mass transfer coefficient at 20 °C; $(k_La)_{U_G}$, volumetric mass transfer coefficient obtained with U_G; $(k_La)_\mu$, volumetric mass transfer coefficient obtained with a liquid phase with μ; m, Cross rate constant; Re, Reynolds number; U_G, superficial gas velocity; t_f, characteristic time of the mass transfer; U_{trans}, transition superficial gas velocity between bubbly and churn-turbulent flow regimes; V, volume of liquid inside of the bubble column; ζ, probe's response time; μ, dynamic viscosity; μ_a, dynamic apparent viscosity; $(\mu_a)_{av}$, average dynamic apparent viscosity; μ_0, zero shear viscosity; $\dot{\Upsilon}$, shear rate; $\dot{\Upsilon}_{av}$, average shear rate.

* Corresponding author. Tel.: +44 (0)1234 758366.
E-mail address: E.Cartmell@cranfield.ac.uk (E. Cartmell).

http://dx.doi.org/10.1016/j.cej.2015.03.051
1385-8947/

considered a fluid of complex matrix exhibiting pseudoplastic rheological behaviour [6,7], with its apparent viscosity (μ_a) being highly affected by temperature [8], solid content [9–11] or shear history [12]. Typical apparent viscosities of such sludges are commonly thought to range between 150 and 400 cPo (based on a 2–4% total solid content) although ranges as wide as 50–1000 cPo have been reported (Table 1). This μ_a variability and complex rheology challenges mass transfer process design based on empirical correlations obtained for Newtonian fluids and necessitates an understanding of the impact that viscous and rheological variations can have in process performance.

Increased μ_a has consistently been reported to lead to mass transfer retardation [13] and its impact reported in terms of volumetric mass transfer coefficient (k_La) reduction. However, gas to liquid mass transfer in viscous fluids is still poorly understood, particularly when considering fluids with non-Newtonian rheological behaviour [14]. Although different fluids have been investigated, the comparison between studies in order to gain a broad understanding of the importance of μ_a and rheology on k_La is limited, due to the dependence of k_La on experimental set-up and considerations used for its calculation. Sparger type [15], probe position [16], probe dynamics [16], assumptions for calculation [16] and data truncation [17] can substantially affect k_La. This necessitates the development of studies that address the impact on mass transfer of μ_a, rheological behaviour and operational conditions with a single experimental set-up and reported assumptions for calculations.

The gap in knowledge is further evidenced when the reasons behind the impact of μ_a on mass transfer are considered. Several mechanisms have been proposed in the literature, such as poorer gas distribution [13], formation of larger bubbles [18], reduced bubble breakup due to a higher stability [19], higher resistance for gas to liquid transfer [2], reduced coalescence efficiency due to a lower drainage velocity of the liquid film between bubbles [14], reduced bubble oscillation [14] or increased residence time [20]. Several of these mechanisms are dependent on the hydrodynamics inside of the bubble column, which have been reported as key for understanding mass transfer in multiphase reactors [21,22]. The transition superficial gas velocity (U_{trans}) between bubbly and churn-turbulent flow regimes has been reported of particular interest to understand mass transfer [23]. However, the effect of liquid μ_a and rheology in U_{trans} has not been extensively investigated so far [21]. A better understanding is hence required to achieve a better design and process operation in industrial sectors where the performance of gas to liquid mass transfer systems can be hindered by μ_a variations.

This paper assessed the impact of μ_a on CO_2 gas to liquid mass transfer and hydrodynamics for fluids of different rheologies (Newtonian and non-Newtonian), with a single experimental set-up and reported assumptions for k_La calculations. Absorption tests with varied μ_a, rheologies and gas flowrates were performed in a high aspect ratio bubble column, where k_La and flow regime patterns were investigated while considering dissolved gas measuring probe dynamics. Results are discussed in the basis of differences between fluids of varied rheologies and particularised for those conditions imitating the behaviour of anaerobically digested sewage sludge.

2. Materials and methods

2.1. Fluids selection and solutions preparation for the absorption tests

Absorption tests with liquid phases of different μ_a and rheological behaviours were performed, including those operational conditions mimicking the operation of ADs. The fluids to be used were selected based on having different rheologies, published μ_a data availability and stable μ_a to pH variations. Glycerol (⩾98%; Fisher Scientific, Loughborough, UK) and carboxymethyl cellulose sodium salt (CMC) (M_W = 700,000; Sigma–Aldrich, Dorset, UK) were chosen as Newtonian and non-Newtonian fluids, respectively. The μ_a of the solutions tested was obtained from the studies of Segur and Oberstar [22] and Eshtiaghi et al. [6] for glycerol and CMC, respectively. CMC solutions with high polymer concentration (>1%) can exhibit a shear thickening or shear thinning behaviour as a function of shear rate ($\dot{\Upsilon}$) [24]. In this study conditions in the shear thinning range were utilised, where rheological properties can be modelled with the simplified Cross viscosity model (Eq. (1)) [6]. Suitable parameters to be used in the Cross viscosity model for solutions with different CMC concentration can be consulted in the work of Eshtiaghi et al. [6]. CMC was selected because it suitably mimics the rheological properties of digested sludge in steady state at high shear rates ($\dot{\Upsilon} > 20\ s^{-1}$) [6]. The rheological behaviour of a CMC solution is conditioned by the molecular weight and the concentration of the polymer used to generate that solution [25]. In order to ensure that data could be extrapolated between studies, CMC with the same molecular weight and from the same supplier (M_W = 700,000 g mol^{-1}; Sigma–Aldrich, Dorset, UK) as Eshtiaghi et al. [6] was used.

$$\mu = \frac{\mu_0}{1 + K\dot{\Upsilon}^m} \quad (1)$$

where μ_0, zero shear viscosity; K, consistency index; $\dot{\Upsilon}$, shear rate; m, Cross rate constant.

The solutions to be used in the absorption tests were prepared by dissolving the correct amount of chemical in deionized (DI) water at room temperature. The CMC solutions were prepared under continuous stirring at 300–400 rpm using a RW20 digital

Table 1
Rheological properties and viscosities reported for sludge. Where TS, total solids; SRT, solids retention time; SS, suspended solids.

References	Material	Material characterisation	Fluid behaviour	μ_a (cPo)	Conditions
[10]	Digested sludge	TS = 2.3% SRT = 58 d	Pseudoplastic	200–400 cPo	
[9]	Fermented sludge	TS = 4%	Pseudo-plastic thixotrophic	⩽150 cPo	T = 25 °C $\dot{\Upsilon} = 36.71\ s^{-1}$
[39]	Liquid manure	2.5% ⩽ TS ⩽ 12.1%	Pseudoplastic (if TS ⩾ 2.5%)	– 6–8 cPo if TS = 2.5% – 10–30 cPo if TS = 5.4% – 250–2930 cPo if TS = 12.1%	T = 35 °C
[38]	Anaerobically digested sludge	SS = 24 kg m^{-3}		37–406 cPo	
[6]	Thickened digested sludge	TS = 3.23%		50–1000 cPo	T = 25 °C
[11]	Anaerobically digested sludge	2% ⩽ TS ⩽ 8%	Pseudoplastic thixotrophic	– ⩽310 cPo if TS ⩽ 4% – 310–625 cPo if TS = 4–5%	μ_a at 30 rpm

paddle stirrer (IKA, Staufen, Germany). Any CMC aggregate was dissolved by stirring the solution at 200–250 rpm overnight.

2.2. Absorption experimental rig description

A high aspect ratio bubble column (2 m tall and 10.1 cm diameter) was used to develop CO_2 absorption tests (Fig. 1). The column was filled up to 1.7 m with the liquid phase. A manifold divided the incoming gas stream into seven inlets, which were connected to a perforated plate placed at the bottom of the column. A metallic mesh with 0.5 mm hole size was mounted on top of the plate, acting as a finer diffuser. CO_2(g) was used for the absorption tests and N_2(g) was bubbled between replicates to achieve full desorption of the CO_2. A sufficient resting time was allowed for any bubbles entrapped in the liquid phase to be removed. N_2(g) and CO_2(g) were supplied from gas cylinders (BOC, Manchester, United Kingdom) and their flowrate regulated by mass flow controllers (MFC) (Premier Control Technologies, Norfolk, United Kingdom). The free CO_2 concentration in the liquid phase was monitored using an InPro5000(i) dissolved CO_2 sensor (Mettler Toledo Ltd., Leicester, UK) installed in the centre of the cross sectional area at 1.5 m from the diffusion mesh and connected to a Multi-parameter Transmitter M400 (Mettler Toledo Ltd., Leicester, UK). Each absorption test was developed at least in duplicates and in triplicates in the majority of the cases.

The characteristics of the liquid phases and operational conditions (superficial gas velocities (U_G) and associated average shear rates ($\dot{\Upsilon}_{av}$) obtained with Eq. (2) [26]) used in the absorption tests are compiled in Table 2.

$$\dot{\Upsilon}_{av} = 50 \cdot U_G \tag{2}$$

where U_G is the superficial gas velocity in cm s^{-1}.

A flow regime map for DI water:glycerol solutions was obtained by observation of the hydrodynamics in the column for each μ_a tested, for U_G between 0.16 and 3.7 cm s^{-1} increased with a step of 0.2 cm s^{-1}. Flow regimes were categorised as imperfect bubbly, churn-turbulent or slug flow as described by Kantarci et al. [21] and Cheng et al. [27]. The gradual transition between regimes for increasing U_G [23] was categorised as a transition range. The U_{trans}, considered for the first U_G leading to churn-turbulent flow regime, was also determined for all the liquid phases tested.

2.3. Considerations for the calculation of volumetric mass transfer coefficients

The calculation of k_La from CO_2 absorption tests was based on the iterative resolution of Eq. (5). This equation was obtained from the combination of the two film theory by Lewis and Whitman (Eq. (3)) and that modelling the response time of the probe (ζ) as a first order process (Eq. (4)). Eq. (5) has been widely used in this or equivalent forms in the literature [16,28], when the probe's dynamics cannot be neglected. Consideration of the probe dynamics was necessary since the characteristic time of the mass transfer $t_f = (k_La)^{-1}$ did not meet the criterion $t_f > 10\zeta$ [16]. An average ζ of 91.5 s was identified as suitable for all the conditions tested. This was measured as the time required to reach 63% of the final solubility when submitted to a step change in CO_2 concentration [29].

$$\frac{dC}{dt} = k_La(C^* - C) \tag{3}$$

$$\frac{dC_{sensor}}{dt} = \frac{(C - C_{sensor})}{\zeta} \tag{4}$$

$$C_{sensor} = C^* + \frac{C^* - C_0}{1 - \zeta k_La} \cdot \left[\zeta k_La \cdot \exp\left(\frac{-t}{\zeta}\right) - \exp(-k_La \cdot t)\right] \tag{5}$$

where C, concentration in the liquid phase; C^*, solubility as equilibrium CO_2 concentration at infinite time; C_0, concentration at time cero; C_{sensor}, concentration measured by the probe; k_La, volumetric mass transfer coefficient; ζ, probe's response time.

The impact on mass transfer of other species of the bicarbonate equilibrium apart from dissolved CO_2 was negligible, since the pH was below 5.9 at the end of all the absorption tests performed [29]. The impact that CO_2 depletion on the gas phase has on k_La was

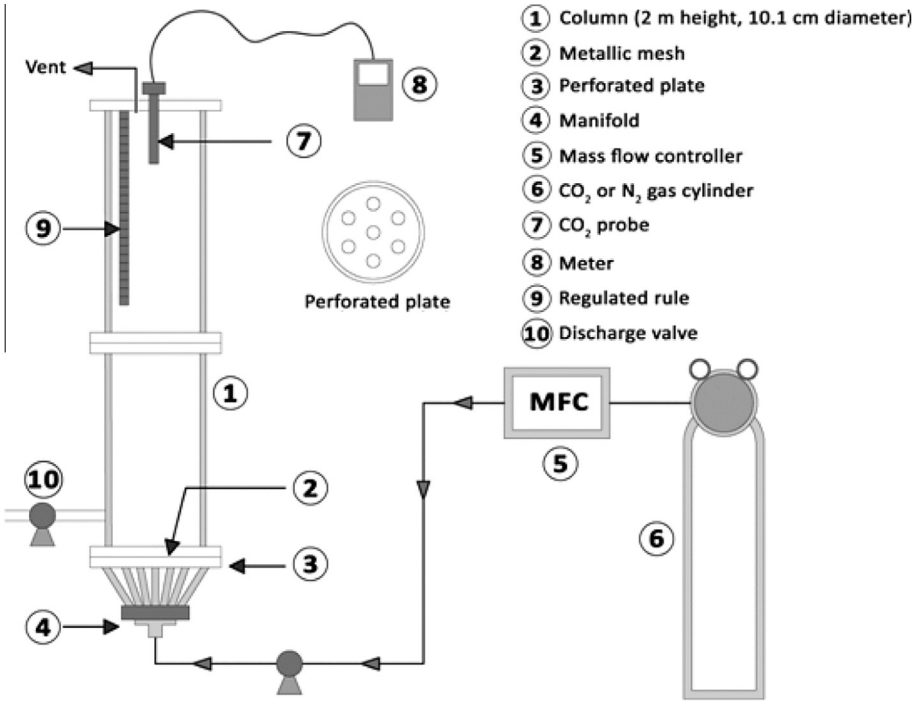

Fig. 1. Set-up of the pilot scale bubble column used for absorption tests.

Table 2
Operational conditions used in the absorption tests.

	U_G (cm s^{-1})					
	0.61		1.73		2.85	
	$\dot{\Upsilon}_{av}$ (s^{-1})					
	30.5		86.5		142.5	
	Concentration (% weight)	μ_a (cPo) at T of test	Concentration (% weight)	μ_a (cPo) at T of test	Concentration (% weight)	μ_a (cPo) at T of test
Glycerol	0	0.9	0	1.0	0	0.9
	10	1.4	10	1.3	10	1.4
	30	2.4	30	2.4	30	2.4
	50	5.8	50	5.7	50	6.2
	70	22.1	70	23.3	70	24.4
	87	124	87	115	87	120
	90	215	90	229	90	219
CMC	0.5	200	0.5	140	0.5	130
	1.0	710	1.0	420	1.0	340
	1.5	1900	1.5	900	1.5	650

Note: Differences in μ of solutions of same glycerol concentration are due to correction as per the temperature of each test.

considered to be offset with the axial pressure variation in the column [16]. Experimental data between 20% and 98% of the final solubility were used for k_La determination [16,17]. This truncation discarded the data with a higher ratio of signal to noise [17] and is in accordance with the literature recommendation of a 30% maximum truncation of the total saturation value [17,30]. It was evident that the adjustment between the second order mass transfer model (Eq. (5)) and the real experimental data was higher if the first part of the data set was discarded (Fig. 2), being the error defined as per Eq. (6). The k_La values were corrected to 20 °C with Eq. (7), considering a value of c of 1.0192 [31].

$$Error = \frac{ABS(C_{model} - C_{sensor})}{C_{sensor}} \times 100 \quad (6)$$

$$(k_La)_{20} = \frac{(k_La)_T}{c^{(T-20)}} \quad (7)$$

where C_{model}, concentration estimated with Eq. (5); C_{sensor}, concentration measured by the probe; $(k_La)_T$, volumetric mass transfer coefficient at temperature T; $(k_La)_{20}$, volumetric mass transfer coefficient at 20 °C.

The results are reported as per alpha (α) and theta factors (θ). Alpha factor (Eq. (8)) was defined as a parameter to assess the impact of μ_a in mass transfer, when normalised against DI water. Theta factor (Eq. (9)) was stated as a parameter to assess the impact of U_G, when normalised against the lowest one tested in the saturation tests: 0.61 cm s^{-1}.

$$\alpha = \frac{(k_La_\mu)_{20\,°C}}{(k_La_{water})_{20\,°C}} \quad (8)$$

$$\theta = \frac{\left((k_La)_{U_G}\right)_{20\,°C}}{\left((k_La)_{0.61}\right)_{20\,°C}} \quad (9)$$

where $(k_La)_{U_G}$, volumetric mass transfer coefficient obtained with U_G, $(k_La)_\mu$, volumetric mass transfer coefficient obtained with a liquid phase with μ.

3. Results and discussion

3.1. Impact of viscosity and superficial gas velocity on mass transfer

A significant reduction of k_La with μ_a was observed for the two fluids and all the operational conditions tested. The relationship between μ_a and k_La was non linear, with the normalised decrease of k_La per μ_a increase ($\Delta k_La/\Delta\mu_a$) being lower at higher μ_a of the liquid phase (Fig. 3). To illustrate, for absorption tests in glycerol solutions with medium U_G (1.73 cm s^{-1}), an increase of 114 cPo in μ from 1.01 to 115 cPo led to a reduction of 96% in k_La (α = 0.04), while a comparable raise from 115 to 229 cPo generated a reduction of 52% (α = 0.02) (Fig. 3a). Similarly, k_La was reduced by 94% (α = 0.06) with an increase of μ_a from 0.92 to 130 cPo in tests with CMC solutions at high U_G (2.85 cm s^{-1}), while an increase from 130 to 340 cPo reduced k_La by 43% (α = 0.04).

The impact of μ_a in k_La was greater with higher U_G, both for CMC and glycerol, as evidenced by the lower alpha factor obtained with increasing U_G for a given liquid μ_a (Fig. 3). For glycerol solutions with a μ of *ca.* 120 cPo (87% glycerol), alpha factors of 0.05, 0.04 and 0.02 were obtained for U_G of 0.61, 1.73 and 2.85 cm s^{-1}, respectively. For equivalent μ_a ranges in CMC solutions (i.e. 0.5%

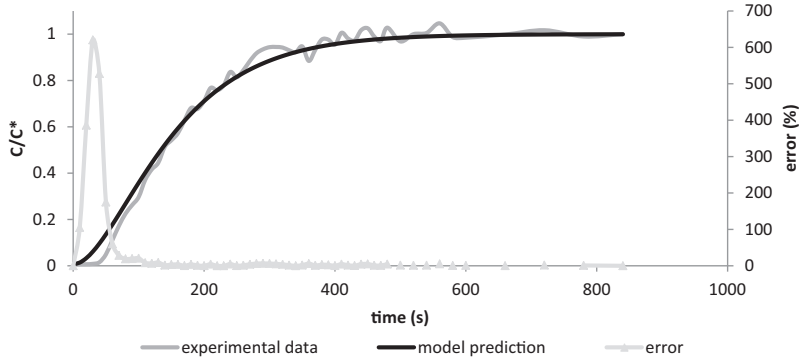

Fig. 2. Example of absorption experimental data and adjustment of model obtained with Eq. (2). Error is defined as per Eq. (5). Data corresponding to a 30% weight glycerol solution saturated with CO_2(g) at medium U_G = 1.73 cm s^{-1}.

CMC) alpha factors of 0.18, 0.13 and 0.06 were obtained for increasing U_G of 0.61, 1.73 and 2.85 cm s^{-1}. The higher impact of μ_a experienced when operating with higher U_G was attributed to variations in the flow regime inside of the system, as explained below (Fig. 4).

When comparing different CMC solutions of close μ_a, a lower alpha factor was obtained for increasing CMC concentrations. Alpha was 0.03 for absorption tests performed in 1.5% CMC solutions with U_G of 2.85 cm s^{-1} (650 cPo) and 0.12 for 1.0% CMC solutions bubbled with U_G of 0.61 cm s^{-1} (710 cPo) (Fig. 3). This indicates a higher negative impact of μ_a for increased CMC concentrations and was attributable to an alteration of bubble shape, increased viscoelastic behaviour and to mass transfer being affected by the μ of the fluid at rest (as opposed to by μ_a determined with $\dot{\Upsilon}_{av}$). These aspects offered a greater resistance to CO_2 gas to liquid transfer [2] and affected fluid hydrodynamics as explained below.

As far as gas flowrate is concerned, an increase in U_G enhanced mass transfer for all the experimental conditions tested, being the benefits (reported as θ) higher for lower μ_a of the liquid phase (Fig. 5). For DI water tests (μ of 0.9–1 cPo) theta factor was 3.1 and 7.1 for medium (1.73 cm s^{-1}) and high U_G (2.85 cm s^{-1}), respectively. For glycerol solutions with a μ of *ca.* 115 cPo (i.e. 87% glycerol), theta factor was 2.1 and 2.3 for medium and high U_G, respectively. An increase in U_G led to formation of bigger and more numerous bubbles and to a higher turbulence inside of the column (Fig. 4). The enhanced mass transfer obtained for increasing U_G (Fig. 5), suggests that the impact of the effects positively affecting k_La (number of bubbles and higher turbulence) was greater than that hindering process efficiency (reduced specific surface area per bubble). The reduced benefit obtained when increasing U_G through liquid phases of higher μ_a (Fig. 5) was attributed to a greater part of the bubbles' oscillation energy being dispersed as viscous dissipation [14], which lead to a reduced turbulence and flow regimes less efficient for mass transfer as described below.

Similar trends of enhanced mass transfer for higher U_G and reduced benefits at higher μ_a of the liquid phase were obtained for CMC solutions (Fig. 5b). Theta was 2.2 and 2.5 for 0.5% CMC solutions (130–140 cPo) as opposed to the 3.1 and 7.1 values recorded for DI water (1.0 cPo), with medium and high U_G (1.73 and 2.85 cm s^{-1}), respectively. However, an irregularity in the trend was observed for the highest CMC concentration tested (650–1900 cPo). Theta factors of 1.7 and 2.2 were obtained for

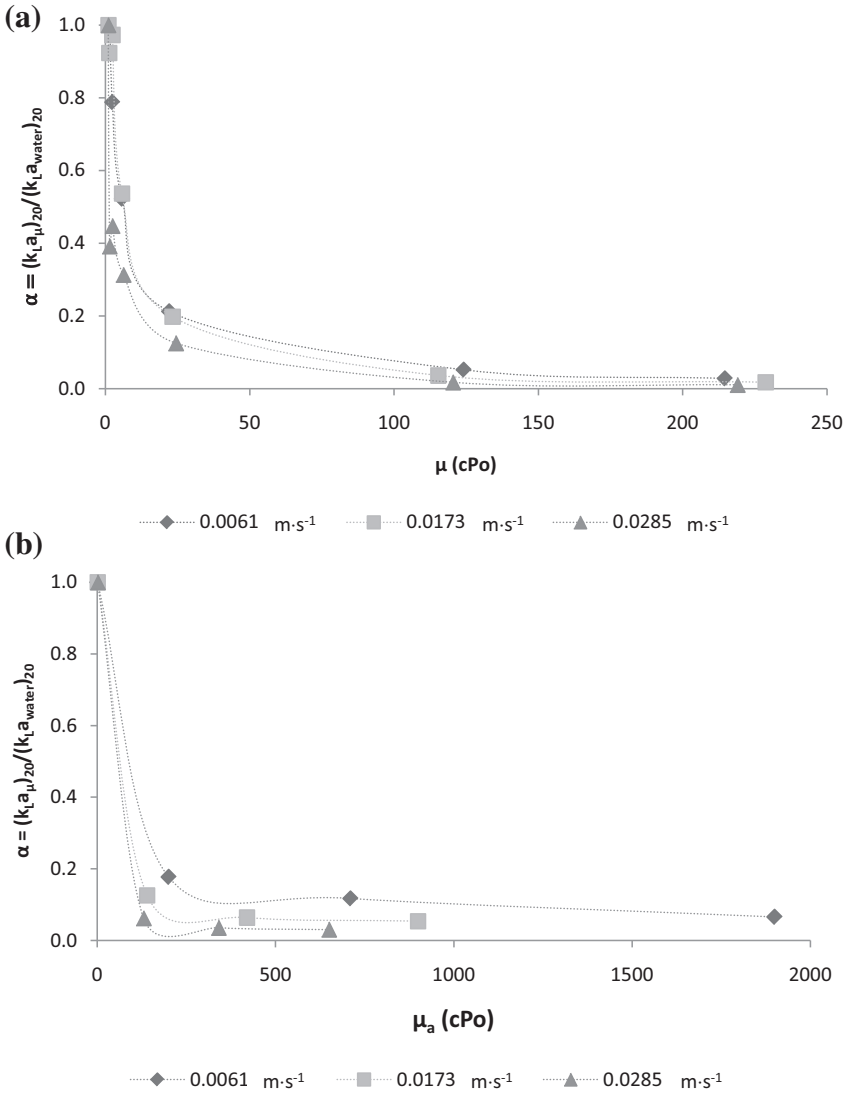

Fig. 3. Impact of μ_a on k_La for (a) DI water:glycerol solutions and (b) DI water:CMC solutions.

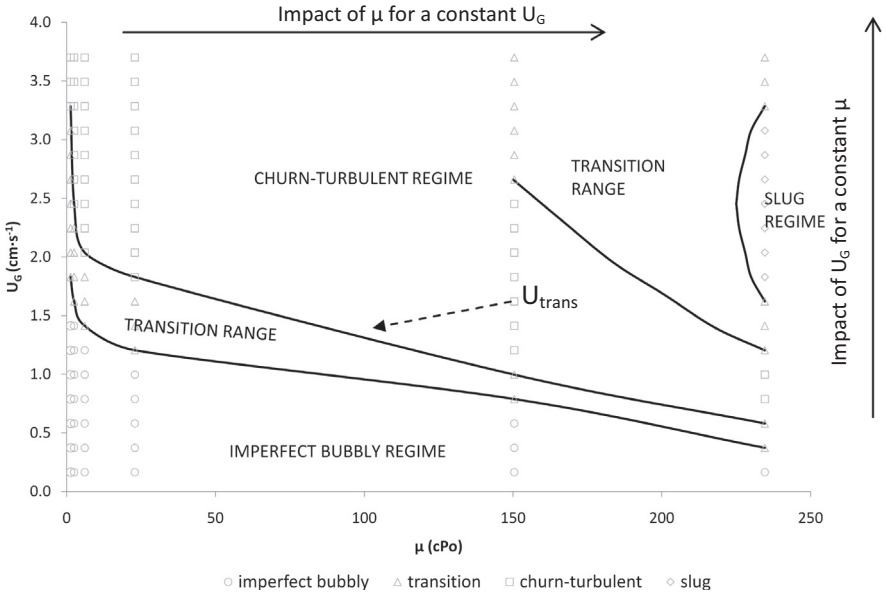

Fig. 4. Flow regime map for DI water:glycerol solutions of different viscosities. Obtained in a bubble column of 10.1 cm diameter and 2 m height.

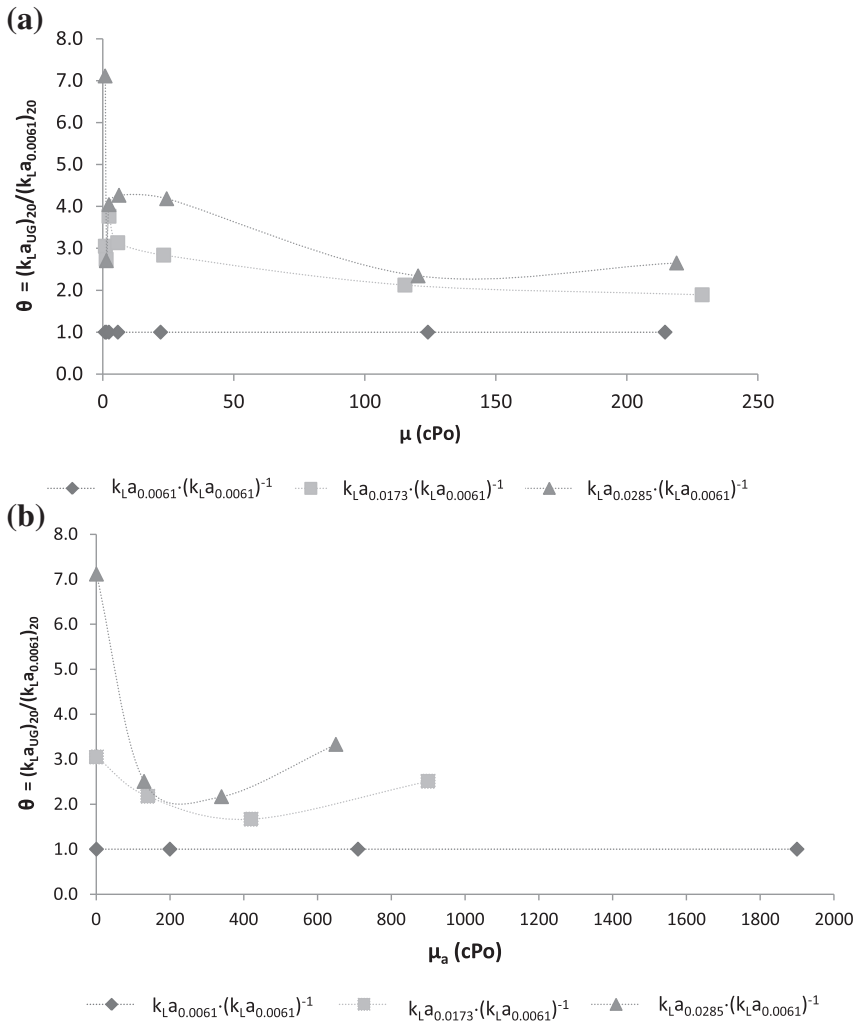

Fig. 5. Impact of U_G on k_La for (a) DI water:glycerol solutions and (b) DI water:CMC solutions. Values normalised with the lowest U_G used in the absorption tests (U_G = 0.61 cm s^{-1}).

1.0% CMC solutions (340–710 cPo) for medium (1.73 cm s^{-1}) and high (1.73 cm s^{-1}) U_G, respectively (Fig. 5b), while significantly higher values (2.5 and 3.3, respectively) were recorded for 1.5% CMC solutions (650–1900 cPo).

3.2. Impact of viscosity and superficial gas velocity on hydrodynamics

Hydrodynamics in bubble columns strongly influence mass transfer [21,23] and hence need to be further understood in relation to μ_a and rheological variations. For comparable μ_a between the Newtonian and non-Newtonian fluids tested, like CMC 0.5% with low U_G and glycerol 90%, the flow regime inside of the column was similar (transition to churn-turbulent). However, bubble size was bigger for CMC solutions (greater *z*-component), which indicated that bubble size was affected by the non-Newtonicity of the CMC solutions with the μ of the fluid at rest influencing the minimum bubble buoyancy required for detachment.

A significant variation in the hydrodynamics inside of the bubble column was observed when μ_a or U_G were changed. Imperfect bubbly, churn-turbulent and slug flow regimes were identified as defined by Bouaifi et al. [30] and the boundaries between them in glycerol solutions compiled in a flow regime map (Fig. 4). At low U_G (<0.37 cm s^{-1}) imperfect bubbly regime was maintained irrespective of μ, although a reduction on the number of bubbles and bigger bubble size was observed for increasing μ when maintaining a constant U_G. An increase in U_G deviated the pattern towards transition regime, where the initial homogeneous flow was disturbed and a more intense turbulence was observed. The U_G leading to transition regime was reduced with increasing μ of the liquid phase, varying between 1.89 and 0.37 cm s^{-1} for glycerol solutions with μ of 1.4 and 235 cPo, respectively. A further increase in U_G led to fully developed churn-turbulent regime, with U_{trans} being dependent on the μ of the liquid phase. Fully developed churn-turbulent regime was observed with $U_G > U_{trans}$ = 3.1 cm s^{-1} for glycerol solutions with μ of 1.3 cPo (10% glycerol) and with values as low as $U_G > U_{trans}$ = 0.79 cm s^{-1} for glycerol solutions with μ of 234 cPo (90% glycerol).

For μ < 124 cPo (87% glycerol) a further increase in U_G led to an increased level of turbulence without deviating the flow regime from churn-turbulent. At higher liquid μ ($\geqslant$124 cPo) a new transition range was observed, which was characterised by slug bubbles occupying all the column cross sectional area but presenting a high instability (Fig. 6a). For the highest μ tested for glycerol (*ca.* 230 cPo) fully developed slug flow regime was obtained in the top part of the column with U_G from 1.6 to 3.3 cm s^{-1} (Fig. 6b). Further increases of gas flowrate lead to breakage of the slug bubbles and a transition flow with mixed characteristics of slug flow and churn-turbulent regimes.

Similarly, for 0.5% CMC solutions imperfect bubbly regime was observed inside of the bubble column for low U_G ($\leqslant$0.58 cm s^{-1}), while transition and churn-turbulent flows were observed when increasing U_G. Fully developed churn-turbulent regime was observed for $U_G > U_{trans}$ = 0.996 cm s^{-1}, which is close to the values obtained for glycerol with similar μ_a (87% glycerol, Fig. 4). For 1.0% CMC solutions with $U_G \leqslant$ 2.24 cm s^{-1} and 1.5% CMC solutions with $U_G \leqslant$ 3.28 cm s^{-1} the bubbles generated at the bottom of the column merged into bigger bubbles and led to a single raising chain in the centre of the column, without a variation of flow regime being observed for the experimental conditions tested. A lack of oscillation for single bubbles rising in stagnant CMC solutions has been previously reported [32] and associated with the solutions' high μ_a [33], which leads to a great level of viscous dissipation. The volume active for mass transfer appeared to be limited to the central plume of raising bubbles, with non-mixed areas of higher μ_a in the outer annulus. Conventional slug flow (slugs covering all the cross sectional area of the column) was reached for $U_G \geqslant$ 2.45 cm s^{-1} in the case of 1.0% CMC solutions and for $U_G \geqslant$ 3.49 cm s^{-1} in tests performed in 1.5% CMC solutions.

The regime observed for 1.0% CMC solutions with $U_G \leqslant$ 2.24 cm s^{-1} and 1.5% CMC solutions with $U_G \leqslant$ 3.28 cm s^{-1} can be named as slug–annular flow (Fig. 6c), where oblate ellipsoidal caps, skirted or inverted tear drop shaped bubbles (Fig. 7) were effectively stabilised by the non-mixed fluid in the outer annulus, which appeared to apply a dragging force imitating a wall effect. The slug–annular flow found in this study partly resembles the pseudo-slug flow described in horizontal pipes, where a continuous liquid film is formed on the pipe wall and slugs touching the top of the pipe are only formed occasionally, being the gas stream normally confined within the pipe's core [34,35]. However, the analogy is limited since gravity leads to a non-symmetric flow pattern in horizontal pipes while axisymmetric flow pattern can be considered in vertical systems [34]. Besides, the slugs formed in pseudo-slug flow in horizontal pipes tend to have a temporal nature [36], while slugs observed in this study travelled the majority of the column height without significant disturbances. Annular regime has previously been described for vertical tubes [35]. However, the gas phase was previously envisaged as continuous and the liquid as partly dispersed [34]. The new slug–annular flow described in this study is characterised by liquid occupying the entire column but being divided into two separate regions: outer stagnant annulus and liquid contained in the centre of the column, being the latest disturbed only by ascendant slugs of gas (Fig. 6c). Small stagnant gas bubbles were found entrapped in the external annulus close to the column wall, which further confirmed that non-mixed areas with scarce contribution to mass transfer were present. The inner part of the bubble column was characterised by $\dot{\Upsilon} > \dot{\Upsilon}_{av}$ and μ_a lower than that predicted with $\dot{\Upsilon}_{av}$ (Fig. 6c), while the stagnant liquid areas found in the outer annulus where subjected to a $\dot{\Upsilon} < \dot{\Upsilon}_{av}$ that lead to μ_a higher than in the bulk of the fluid. A non-uniform $\dot{\Upsilon}$ and μ_a distribution in the cross sectional area of bubble columns with CMC solutions was previously reported by Nishikawa et al. [37] for U_G < 4 cm s^{-1} when studying heat transfer.

In slug–annular regime bubble size and bubble shape were conditioned by both U_G and μ_a. In 1.0% CMC solutions oblate ellipsoidal caps with a short tail were observed (Fig. 7a), which progressively transformed into skirted bubbles when U_G was increased (Fig. 7e). Quasi spherical shaped bubbles with a short tail (inverted tear drop) were characteristic of 1.5% CMC solutions, with an increase in U_G leading to bigger bubbles (reduced outer annulus) with similar shape (Fig. 7). The difference in bubble shape observed for CMC solutions of different concentrations was believed associated with the increased elastic behaviour of the solutions at higher polymer concentrations. An increase in bubble size in Newtonian fluids has been reported to progressively alter bubble shape from spherical to oblate ellipsoidal to spherical cap [38]. However, bubbles ascending in viscoelastic fluids present an inverted tear drop shape because a negative wake is formed behind the bubble [38]. Benchabane and Bekkour [24] reported a critical CMC concentration of 2.5% below which a viscous behaviour is expected and above which elasticity gains importance. However, this transition between rheology models was observed to be progressive, with an increased CMC concentration leading to higher deviations from viscous behaviour. The evolution in bubble shape observed in 1.0% CMC solutions (Fig. 7a, c and e) was hence characteristic of Newtonian fluids [38] and indicated that the solution presented a predominantly viscous behaviour. However, the inverted tear drop shape observed in 1.5% CMC solutions (Fig. 7b, d and f) evidenced the importance of elasticity at higher CMC concentrations.

The described evolution in bubble shape could be further explained attending to dimensionless numbers. The oblate

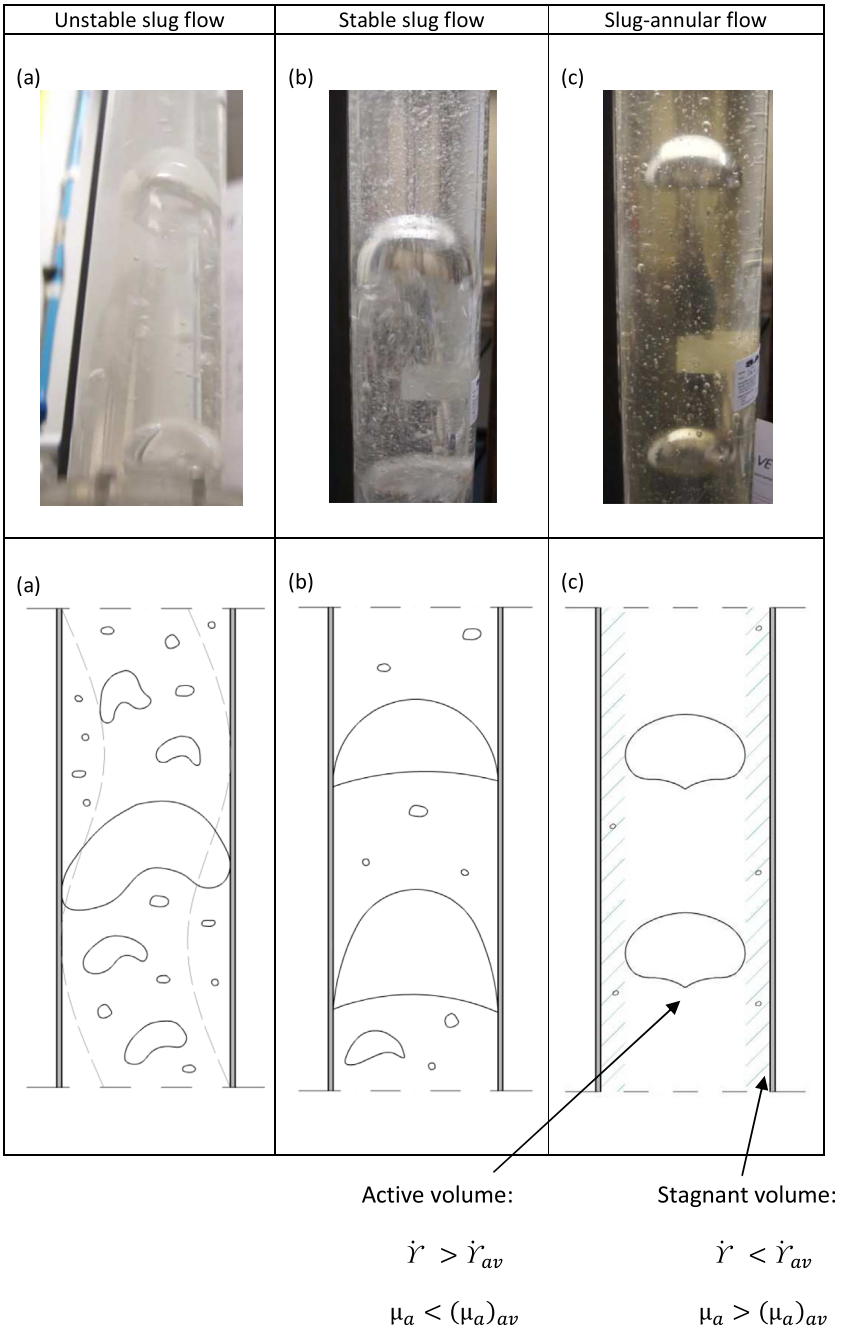

Fig. 6. Types of slug flow regimes observed: (a) unstable slug flow or transition between churn-turbulent and slug flow regimes observed for 87% glycerol solutions with U_G = 2.45 cm s^{-1} (μ = 124 cPo), (b) stable slug flow observed for 90% glycerol solutions with U_G = 1.83 cm s^{-1} (μ_a = 220 cPo) and (c) slug–annular flow observed for 1.0% CMC solutions with U_G = 1.62 cm s^{-1}.

ellipsoidal shape observed for lower $\dot{\Upsilon}$ (lower Reynolds number (*Re*)) (Fig. 7a) and the skirted bubble shape pictured at high $\dot{\Upsilon}$ (Fig. 7e) are in agreement with previous literature. Bhaga and Weber [39] described oblate ellipsoidal bubbles formed at low *Re* numbers and spherical caps at $Re \geqslant 45$. Clift et al. [40] reported a correlation between bubble shape and dimensionless numbers, which evidenced that spherical caps are characteristic of conditions with high *Re* and *Eötvös* numbers (e.g. Fig. 7e).

When different CMC solutions of similar μ_a are compared, a bigger bubble size was observed for the highest CMC concentration. Fig. 7(a) and (f) evidences the presence of bigger bubbles for tests with 1.5% CMC solutions at high U_G (μ_a = 650 cPo) than for 1.0% CMC at low U_G (μ_a = 710 cPo), being the bubbles flatter for reduced CMC concentrations. Part of this difference in bubble size could be attributed to the higher gas flowrate required with 1.5% CMC solutions to achieve a μ_a comparable to 1.0% CMC (shear thinning fluid). However, bubble volume was considerably bigger for higher CMC concentrations even when an equivalent U_G was applied (Fig. 7a, c and e VS Fig. 7b, d and f). Bubbles formed in solutions of higher CMC concentration consistently presented a higher vertical component ($c > a$ in Fig. 7), which was attributed to the described impact of viscoelasticity in bubble shape and to the influence of the μ of the fluid at rest in buoyancy for detachment. In unmixed shear thinning fluids (e.g. CMC), the at rest μ appears

1.0% CMC image	1.0% CMC schema	1.5% CMC image	1.5% CMC schema	U_G ($cm \cdot s^{-1}$)
(a) 	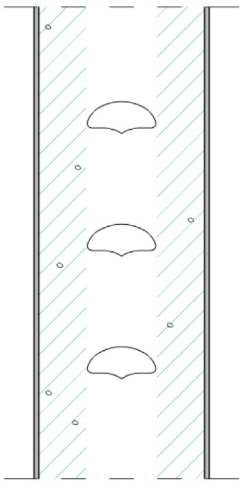	(b) 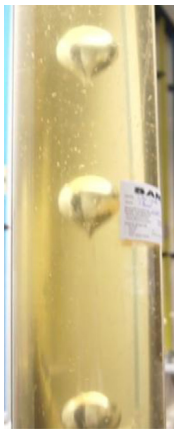	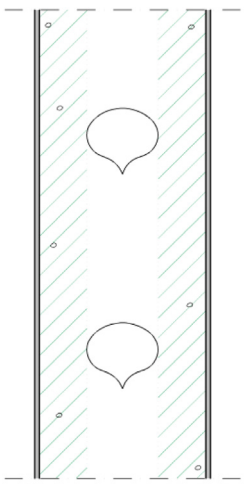	0.58
(c) 	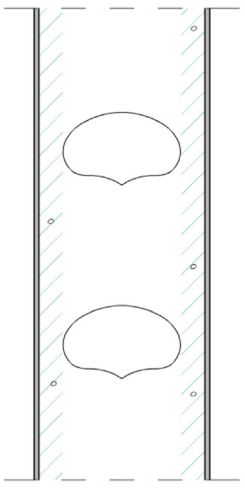	(d) 	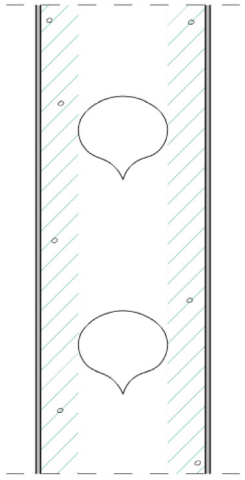	1.62
(e) 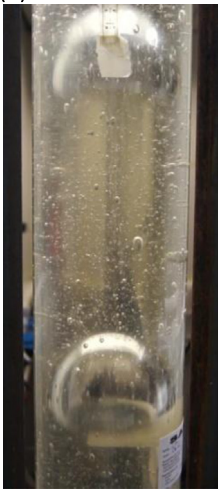	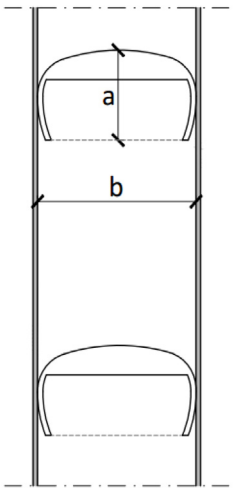	(f) 	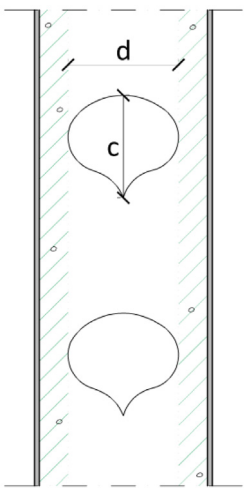	2.87 $a < c$ $b > d$

Fig. 7. Bubble shape, bubble size and evolution of liquid working volume actively used for gas to liquid mass transfer in the slug–annular flow regime observed in shear thinning fluids (1.0% CMC and 1.5% CMC solutions).

to effectively act as a pseudo-yield stress that needs to be overcome by bubble buoyancy. A higher bubble vertical component and reduced cross sectional area lead to a more favourable balance between drag force (function of bubble cross sectional area) and buoyancy (function of bubble volume), which allows the bubble to overcome the opposing forces and rise in a stable plume with a reduced active volume for mass transfer. This concept is in accordance with previous references reporting bubble shape to be influenced by yield stress [41] and with the mathematical simulations of Tsamopoulos et al. [42], which predicted an elongation of the vertical component of bubbles when formed in fluids of increasing yield stress.

The stable plume of rising bubbles of the slug–annular flow allowed a visual observation of the coalescence process for 1.0% and 1.5% CMC solutions. At lower μ_a the rising bubbles collided more frequently with others in a higher position, resulting in coalescence. On the contrary, bubbles formed in 1.5% CMC solutions tended to maintain their relative distance in the vertical chain of bubbles throughout the height of the column and coalescence was not observed apart from that taking place close to the diffusion device. Retardation in the drainage of the liquid film between bubbles for higher μ_a was hence evidenced, which appeared responsible for a reduced bubble coalescence and break-up.

3.3. Mechanistic understanding

Variations of k_La associated with μ_a and rheological changes were related with the influence of these on bubble buoyancy, bubble shape, viscoelasticity, viscous dissipation of bubble oscillation energy (turbulence level), retardation in drainage of liquid film between bubbles (coalesce and break-up) and at rest μ in shear thinning fluids; all of which in turn determined the hydrodynamics in the system. The reduction in mass transfer efficiency associated with a μ_a raise was hence attributed to a combination of effects. The increase in the size of the bubbles formed at higher μ_a implied a reduction of specific surface area with negative implications in k_La [20]. Besides, bubbles tended to coalescence close to the diffusion mesh, leading to bigger bubbles in the bulk of the column and resulting in slug flow or annular-slug flow for some of the higher μ_a tested (Figs. 4 and 7). Slug flow regime is associated with poor mass transfer [43], leading to lower k_La values. Furthermore, higher μ_a led to a reduced turbulence and radial oscillation, due to a partial absorption of oscillation energy as viscous dissipation [14] and limiting the positive impact of turbulence on mass transfer. A flow without radial dispersion was hence observed for the highest μ_a tested, where bubbles appeared stable in a vertical chain and the probability of collision leading to bubble break-up was clearly reduced [14,19]. The higher impact of μ_a in k_La at higher U_G (lower alpha factor for increasing U_G for a given liquid μ_a (Fig. 3)) was again related with the hydrodynamics inside of the bubble column. This can be illustrated with glycerol solutions, where a change of μ for the lowest U_G tested (0.61 cm s^{-1}) did not deviate the flow pattern from imperfect bubbly. On the contrary, at higher U_G, an increase in μ changed the hydrodynamics from imperfect bubbly (<1.4 cPo) to transition regime, churn-turbulent regime and even slug flow (*ca.* 230 cPo). Since slug flow is the least favourable regime for mass transfer [43], the variation of hydrodynamics towards regimes of lower turbulence explains the varied impact of μ for different gas flowrates.

Mass transfer was enhanced with higher U_G, with the benefit being reduced at higher μ_a of the liquid phase both for Newtonian (glycerol) and non-Newtonian (CMC) solutions (Fig. 5b). However, an irregularity in the trend was observed for the highest CMC concentration tested (1.5%), where higher theta factors than for lower concentrations of CMC were obtained (2.5 and 3.3 for U_G of 1.73 cm s^{-1} and 1.73 cm s^{-1}, respectively, for 1.5% CMC solutions and 1.7 and 2.2 for 1.0% CMC). This irregularity was due to the particular implications that the non-Newtonian nature of CMC solutions has in bubble shape (specific surface area, Fig. 7), bubble buoyancy and in the system hydrodynamics. Slug flow was achieved in 1.0% CMC solutions at a lower U_G than for 1.5% CMC solutions, 2.45 and 3.49 cm s^{-1}, respectively. Therefore, for the same U_G = 2.85 cm s^{-1} the bubbles formed in 1.0% CMC solutions were characterised by a higher cross sectional area and a lower vertical component than for 1.5% CMC solutions, where bubbles had a higher *z*-component and stagnant areas characteristic of slug–annular flow were present in the outer annulus of the column (Fig. 6). Consequently, a lower volume of liquid was actively involved in mass transfer for 1.5% CMC solutions, which effectively implied a higher gas rate (amount of gas per liquid volume treated) and hence a greater positive impact of increased U_G in k_La (higher θ). The two liquid regions described in slug–annular flow are visualised as decoupled in terms of mass transfer. While increased k_La are expected in the inner core (higher gas rate), mass transfer in the outer stagnant annulus appeared virtually limited to diffusion mechanisms. It must be considered that the dissolved CO_2 probe was fixed in the centre of the cross sectional area of the bubble column, being the k_La values reported obtained for the area active for mass transfer in the case of slug–annular regime.

3.4. Practical implications for gas to liquid mass transfer in sludge

The conditions that would imitate the common operation of sewage sludge ADs (μ and $\dot{\Upsilon}$) were included within those tested. A range of μ_a of 150–400 cPo was considered to cover the variability observed in digested sludge with a 2–4% total solid content (Table 1) [6,10,11,44]. A range of 50–80 s^{-1} covers the $\dot{\Upsilon}$ most frequently used in design of full scale ADs [11] and was represented by the absorption tests performed at low and medium U_G, $\dot{\Upsilon}_{av} = 30.5\ s^{-1}$ and $\dot{\Upsilon}_{av} = 86.5\ s^{-1}$, respectively. Since CMC has been reported to suitably mimic the rheological properties of digested sludge in steady state at high $\dot{\Upsilon}$ (above 20 s^{-1}) [6], the results of this study give indication of the trends expected when performing mass transfer in digested sludge, for applications such as CO_2 uptake by biotransformation to methane [5] or control of ammonia toxicity in ADs [4].

It was concluded that fluid μ_a and rheology need to be thoroughly characterised and included in the design of any mass transfer system involving digested sludge, since a poor characterisation of these variables can have a double negative implication in the performance of a gas to liquid mass transfer system. On the one hand, a variation of μ_a that has not been accounted for in the design stage, could significantly reduce the performance of the process. A reduction of 43% in k_La was obtained with a μ_a increase from 130 to 340 cPo (0.5 to 1.0% CMC), which is within the reported range of μ_a variability in digested sludge (Table 1). Gas flowrate could be increased as a means to compensate for the reduced performance. Theta factors of 1.7–2.5 were obtained when increasing U_G from 0.61 to 1.73 cm s^{-1} and of 2.2–3.3 when applying 2.85 cm s^{-1} for CMC solutions. However, this required 3–5 times higher gas flowrates, with the associated increased operational costs that may offset the benefits of an enhanced k_La. When assessing μ_a impact in terms of the diffusion system performance, an increase of μ_a from 130 to 340 cPo in CMC solutions implied a reduction in gas transfer rate (GTR) (Eq. (10)) from 31.4 ± 1.4 to 19.0 ± 0.3 mg s^{-1} and in gas transfer efficiency (GTE) (Eq. (11)) from 7.6 ± 0.3% to 1.6 ± 0.1%. Since sewage sludge μ_a is highly influenced by solid content [9] and temperature [8], these

need to be particularly characterised and accounted for since the design stage of a gas to liquid mass transfer system.

$$GTR\ (\mathrm{mg\ s^{-1}}) = (k_La)_{20\ ^\circ C} \cdot (C^* - C) \cdot V \quad (10)$$

$$GTE\ (\%) = SGTR \cdot (\dot{F}_{CO_2})^{-1} \cdot 100 \quad (11)$$

where C, concentration in the liquid phase; C^*, solubility as equilibrium CO_2 concentration at infinite time; $\dot{F}_{CO_2}$, incoming CO_2 mass flow rate; $(k_La)_{20}$, volumetric mass transfer coefficient at 20 °C; V, volume of liquid inside of the bubble column.

On the other hand, this study evidenced the existence of a slug–annular flow in shear thinning fluids with rheological behaviour comparable to that of anaerobically digested sewage sludge (e.g. CMC solutions). In this hydrodynamic regime, slug-like bubbles appeared stabilised by stagnant liquid of high μ_a rather than by the column wall itself, challenging the common statement of slug flow being limited to the operation of laboratory scale bubble columns of small diameter [23]. A stable plume of rising bubbles without radial oscillation and a reduced volume of liquid actively involved in mass transfer were hence observed for 1.0% and 1.5% CMC solutions. The reduced viscous forces in the central part of the column ($\mu_a < (\mu_a)_{av}$) led to higher alpha factors (lower impact of μ_a) for CMC than for glycerol solutions of similar μ_a (Fig. 3), when placing the dissolved CO_2 probe in the centre of the cross sectional area. However, the stagnant areas of reduced mass transfer efficiency present in the outer annulus of the column should be avoided in a full scale operation. In practical terms, the appearance of slug–annular flow in a volume of shear thinning fluid with CO_2 injection could lead to a reduced active volume for mass transfer due to the system operating as several individual bubble columns separated by stagnant areas. Whereas k_La would be higher than predicted in each column core, mass transfer in the outer annulus would be mainly limited to that associated with diffusion mechanisms. In order for this to be avoided, special consideration should be given towards the design of efficient gas distribution systems in mass transfer processes involving digested sludge, with an increased number of diffusion devices per surface area than when dealing with Newtonian fluids of similar μ_a. Alternatively, additional mixing devices capable of disturbing the fluid stagnant areas could be considered.

4. Conclusions

Mass transfer retardation due to increased μ_a was investigated for Newtonian and shear thinning fluids. A non-linear reduction of mass transfer efficiency with increasing μ_a was observed, being the impact higher at low μ_a ranges and high U_G.

The impact of both μ_a and U_G in k_La was predominantly influenced by changes in the system hydrodynamics through an alteration of bubble buoyancy, bubble shape, turbulence level and drainage of the liquid film between bubbles. Slug–annular flow was observed for shear thinning fluids of high μ_a, including rheological conditions imitating digested sewage sludge, where k_La was conditioned by the μ of the fluid at rest and the active liquid volume for mass transfer was reduced because of the presence of a stagnant outer annulus. Particular emphasis should be placed in selecting the number of diffusion systems per unit area to be used in a mass transfer system involving sewage sludge, in order to avoid a reduction in process performance and active volume as a consequence of viscous or rheological variations.

Acknowledgements

This work was sponsored by Severn Trent Water and the Engineering and Physical Sciences Research Council (EPSRC), whose assistance the authors gratefully acknowledge.

References

[1] R.H. Xiong, S.C. Wang, Z. Wang, S.C. Xu, J.X. Wang, Experimental investigation of mass transfer in high viscosity media, Int. Commun. Heat Mass Transf. 30 (2003) 817–824.
[2] A.C. Badino, M.C.R. Facciotti, W. Schmidell, Volumetric oxygen transfer coefficients (k_La) in batch cultivations involving non-Newtonian broths, Biochem. Eng. J. 8 (2001) 111–119.
[3] F. García-Ochoa, E. Castro, V. Santos, Oxygen transfer and uptake rates during xanthan gum production, Enzyme Microb. Technol. 27 (2000) 680–690.
[4] M. Walker, K. Iyer, S. Heaven, C.J. Banks, Ammonia removal in anaerobic digestion by biogas stripping: an evaluation of process alternatives using a first order rate model based on experimental findings, Chem. Eng. J. 178 (2011) 138–145.
[5] Y. Bajón Fernández, A. Soares, R. Villa, P. Vale, E. Cartmell, Carbon capture and biogas enhancement by carbon dioxide enrichment of anaerobic digesters treating sewage sludge or food waste, Bioresour. Technol. 159 (2014) 1–7.
[6] N. Eshtiaghi, S.D. Yap, F. Markis, J.-C. Baudez, P. Slatter, Clear model fluids to emulate the rheological properties of thickened digested sludge, Water Res. 46 (2012) 3014–3022.
[7] J.C. Baudez, F. Markis, N. Eshtiaghi, P. Slatter, The rheological behaviour of anaerobic digested sludge, Water Res. 45 (2011) 5675–5680.
[8] L. Hammadi, A. Ponton, M. Belhadri, Temperature effect on shear flow and thixotropic behavior of residual sludge from wastewater treatment plant, Mech. Time-Depend. Mater. 17 (2012) 401–412.
[9] S.K. Brar, M. Verma, R.D. Tyagi, J.R. Valéro, R.Y. Surampalli, Sludge based *Bacillus thuringiensis* biopesticides: viscosity impacts, Water Res. 39 (2005) 3001–3011.
[10] R. Goel, K. Komatsu, H. Yasui, H. Harada, Process performance and change in sludge characteristics during anaerobic digestion of sewage sludge with ozonation, Water Sci. Technol. 49 (2004) 105–113.
[11] USEPA (United States Environmental Protection Agency), Process Design Manual for Sludge Treatment and Disposal. EPA 625/1-79-011, 1979.
[12] H.C. Honey, W.A. Pretorius, Laminar flow pipe hydraulics of pseudoplastic-thixotropic sewage sludges, Water SA 26 (2000) 19–25.
[13] B. Ozbek, S. Gayik, The studies on the oxygen mass transfer coefficient in a bioreactor, Process Biochem. 36 (2001) 729–741.
[14] M. Martín, F.J. Montes, M.A. Galán, Mass transfer rates from oscillating bubbles in bubble columns operating with viscous fluids, Ind. Eng. Chem. Res. 47 (2008) 9527–9536.
[15] J.J. Heijnen, K. Van't Riet, Mass transfer, mixing and heat transfer phenomena in low viscosity bubble column reactors, Chem. Eng. J. 28 (1984) B21–B42.
[16] B. Gourich, C. Vial, N. El Azher, M. Belhaj Soulami, M. Ziyad, Influence of hydrodynamics and probe response on oxygen mass transfer measurements in a high aspect ratio bubble column reactor: effect of the coalescence behaviour of the liquid phase, Biochem. Eng. J. 39 (2008) 1–14.
[17] J.C. Merchuk, S. Yona, M.H. Siegel, A. Ben Zvi, On the first-order approximation to response of dissolved oxygen electrodes for dynamic k_La estimation, Biotechnol. Bioeng. 35 (1990) 1161–1163.
[18] F. Wicaksana, A.G. Fane, V. Chen, Fibre movement induced by bubbling using submerged hollow fibre membranes, J. Membr. Sci. 271 (2006) 186–195.
[19] P.M. Wilkinson, A. Van Schayk, J.P.M. Spronken, L. Van Dierendonck, The influence of gas density and liquid properties on bubble breakup, Chem. Eng. Sci. 48 (1993) 1213–1226.
[20] A. García-Abuín, D. Gómez-Díaz, J.M. Navaza, Influence of chitosan and chitosan derivatives on hydrodynamics and mass transfer in a bubble contactor, Chem. Eng. Technol. 36 (2013) 596–602.
[21] N. Kantarci, F. Borak, K.O. Ulgen, Bubble column reactors, Process Biochem. 40 (2005) 2263–2283.
[22] J.B. Segur, H.E. Oberstar, Viscosity of glycerol and its aqueous solutions, Ind. Eng. Chem. 43 (1951) 2117–2120.
[23] C.L. Hyndman, F. Larachi, C. Guy, Understanding gas-phase hydrodynamics in bubble columns: a convective model based on kinetic theory, Chem. Eng. Sci. 52 (1997) 63–77.
[24] A. Benchabane, K. Bekkour, Rheological properties of carboxymethyl cellulose (CMC) solutions, Colloid Polym. Sci. 286 (2008) 1173–1180.
[25] W.-M. Kulicket, A.H. Kull, W. Kull, H. Thielking, J. Engelhardt, J.-B. Pannek, Characterization of aqueous carboxymethylcellulose solutions in terms of their molecular structure and its influence on rheological behaviour, Polymer (Guildf) 37 (1996) 2723–2731.
[26] M. Nakanoh, F. Yoshida, Gas absorption by Newtonian and non-Newtonian liquids in a bubble column, Ind. Eng. Chem. Process Des. Dev. 19 (1980) 190–195.
[27] L. Cheng, G. Ribatski, J.R. Thome, Two-phase flow patterns and flow-pattern maps: fundamentals and applications, Appl. Mech. Rev. 61 (2008) 1–28.
[28] K. Van't Riet, Review of measuring methods and results in nonviscous gas–liquid mass transfer in stirred vessels, Ind. Eng. Chem. Process Des. Dev. 18 (1979) 357–364.
[29] P.N.C. Royce, N.F. Thronhill, Estimation of dissolved carbon dioxide concentrations in aerobic fermentations, AIChE J. 37 (1991) 1680–1686.
[30] M. Bouaifi, G. Hebrard, D. Bastoul, M. Roustan, A comparative study of gas hold-up, bubble size, interfacial area and mass transfer coefficients in stirred gas–liquid reactors and bubble columns, Chem. Eng. Process. Process Intensif. 40 (2001) 97–111.
[31] J.K. Bewtra, W.R. Nicholas, L.B. Polkowski, Effect of temperature on oxygen transfer in water, Water Res. 4 (1970) 115–123.

[32] F. Wenyuan, M. Youguang, J. Shaokun, Y. Ke, L. Huaizhi, An experimental investigation for bubble rising in non-newtonian fluids and empirical correlation of drag coefficient, J. Fluids Eng. 132 (2010) 1–7.
[33] S. Li, Y. Ma, S. Jiang, T. Fu, C. Zhu, H.Z. Li, The drag coefficient and the shape for a single bubble rising in non-Newtonian fluids, J. Fluids Eng. 134 (2012) 1–4.
[34] A.K. Jagota, E. Rhodes, D.S. Scott, Mass transfer in upwards co-current gas–liquid annular flow, Chem. Eng. J. 5 (1973) 23–31.
[35] G.F. Hewitt, D.N. Roberts, Studies of Two-Phase Flow Patterns by Simultaneous X-ray and Flash Photography; Report AERE-M 2159, Harwell, 1969.
[36] P.Y. Lin, T.J. Hanratty, Effect of pipe diameter on flow patterns for air–water flow in horizontal pipes, Int. J. Multiph. Flow 13 (1987) 549–563.
[37] M. Nishikawa, H. Kato, K. Hashimoto, Heat transfer in aerated tower filled with non-Newtonian liquid, Ind. Eng. Chem. Process Des. Dev. 16 (1977) 133–137.
[38] N. Dubash, I.A. Frigaard, Propagation and stopping of air bubbles in Carbopol solutions, J. Nonnewton. Fluid Mech. 142 (2007) 123–134.
[39] D. Bhaga, M.E. Weber, Bubbles in viscous liquids: shapes, wakes and velocities, J. Fluid Mech. 105 (1981) 61–85.
[40] R. Clift, J.R. Grace, M.E. Weber, Bubbles, Drops and Particles, Academic Press, London, 1978.
[41] D. Sikorski, H. Tabuteau, J.R. de Bruyn, Motion and shape of bubbles rising through a yield-stress fluid, J. Nonnewton. Fluid Mech. 159 (2009) 10–16.
[42] J. Tsamopoulos, Y. Dimakopoulos, N. Chatzidai, G. Karapetsas, M. Pavlidis, Steady bubble rise and deformation in Newtonian and viscoplastic fluids and conditions for bubble entrapment, J. Fluid Mech. 601 (2008) 123–164.
[43] S.T. Jones, Gas–Liquid Mass Transfer in an External Airlift Loop Reactor for Syngas Fermentation, Iowa State University, 2007.
[44] R.C. Frost, How to Design Sewage Sludge Pumping Systems – TR 185, Stevenage, 1983.